JOURNAL OF GEOPHYSICAL RESEARCH, VOL. 116, D21102, doi:10.1029/2010JD015530, 2011

Origin of the water vapor responsible for the European extreme rainfalls of August 2002: 1. High-resolution simulations and tracking of air masses

G. Gangoiti,[1] E. Sáez de Cámara,[1] L. Alonso,[1] M. Navazo,[1] M. C. Gómez,[1] J. Iza,[1] J. A. García,[1] J. L. Ilardia,[1] and M. M. Millán[2]

Received 23 December 2010; revised 24 June 2011; accepted 12 July 2011; published 3 November 2011.

[1] This article investigates an extreme rainfall event occurred over wide areas of central Europe on August 11–13, 2002. By using a synergistic approach that includes regional modeling, air mass tracking, and observational data sets, the importance of moisture accumulation processes in the Western Mediterranean basin (WMB) is acknowledged as an important mechanism responsible for the magnitude of this event. The RAMS-HYPACT modeling system is used to track air masses from potential marine sources of evaporation. MODIS water vapor products, wind profilers and surface rain gauge measurements are used to substantiate our simulations. Results show that most of the precipitation occurring in central Europe during the initiation of the rainfall episode (August 11) came from vapor accumulated over 4 days (August 6–9) within the WMB: the vapor was transported, after the irruption of the Vb cyclone *Ilse*, through the Italian Peninsula and the Adriatic Sea, into the target area, causing the precipitation episode. On August 12 and 13 the marine sources of evaporation changed to include the north-Atlantic region. The north-African convergence region, the eastern Mediterranean and the Black Sea are revealed to be sources more related to the intense rainfall experienced in eastern Europe. The subsidence-related processes through which pollutants and water vapor can accumulate for several days in the WMB are shown to be very relevant for this event. The quantification of the evaporative sources, responsible for the extreme rainfall events in central Europe, and the relative importance of marine and terrestrial sources within a chosen regional domain are discussed in the companion following article.

Citation: Gangoiti, G., E. Sáez de Cámara, L. Alonso, M. Navazo, M. C. Gómez, J. Iza, J. A. García, J. L. Ilardia, and M. M. Millán (2011), Origin of the water vapor responsible for the European extreme rainfalls of August 2002: 1. High-resolution simulations and tracking of air masses, *J. Geophys. Res.*, *116*, D21102, doi:10.1029/2010JD015530.

1. Introduction

[2] Extraordinary rainfall amounts and intensities were recorded in central Europe during the first half of August 2002. In general, because of the different time response of small and large watersheds, it is very rare that a precipitation event contains the intensity-duration requirements to activate rivers characterized by very different discharge statistics. Concentrated mesoscale events can produce flash floods on small rivers. The exceptionally of the 2002 consists in the fact that flash flooding was first produced on small rivers in Austria, Bohemia, and the Erz Mountains, followed by record-breaking floods in larger rivers: the Vltava, Elbe, and parts of the Danube catchments [*Ulbrich et al.*, 2003a]. These floods caused 36 deaths and over 15 billion USD damage [*Mudelsee et al.*, 2004]. Intense summer precipitations, whether or not they cause river floods, are frequent in central Europe and are associated with a track of cyclones known as 'Vb-track'. According to *Fricke and Kaminski* [2002], the increase in the number of days with extreme precipitation in summer, observed in the long term time series from the Hohenpeissenberg Observatory station in southern Germany (1881–2001), is related to the more frequent occurrence of weather types associated with Vb-tracks. Simulated future scenarios for CO_2-induced climate change show a decrease in total summer rainfall in central Europe and an increase in heavy precipitation events, due to a warmer atmosphere (which can carry more water vapor) and/or an increase in the frequency of this type of cyclone tracks [*Ulbrich et al.*, 2003b; *Christensen and Christensen*, 2003]. During the August 11–13, 2002

[1]Escuela Técnica Superior de Ingeniería de Bilbao, Universidad del País Vasco–Euskal Herriko Unibertsitatea, Bilbao, Spain.
[2]Fundación CEAM, Valencia, Spain.

0148-0227/11/2010JD015530

rainfall episode in central Europe, *Ulbrich et al.* [2003b] showed that back-trajectory analysis point to the Western Mediterranean Basin (WMB) as the main vapor source. Similar conclusions were reported by *James et al.* [2004], but only for the initial stages of the rainfall events.

[3] *Millán et al.* [2005] have drawn attention to a water vapor accumulation excess over the WMB in recent years due to land use changes and increased air pollution; this excess could also explain the observed increase in torrential rains. If the hydrological cycle of the Mediterranean region is being perturbed, it is of key importance to identify the water-vapor evaporation areas responsible for the extreme events and to determine the capacity of the region to recycle its precipitation. In this respect, the HyMeX international program (HYdrological cycle in the Mediterranean EXperiment), launched in 2006 and endorsed by the WMO's two major international programs dealing with weather prediction and climate research (WCRP-THORPEX and WWRP-GEWEX), has focused on understanding the water cycle in this region, with emphasis on high-impact weather events, inter-annual to decadal variability and associated trends in the context of global change. The results should help us to identify both the perturbations of the water cycle in a system with important feedbacks between oceanic, atmospheric, and hydrological processes, and the corrections needed to avoid or reduce extreme rainfall and its consequences.

[4] *Millán et al.* [1997] has demonstrated that the WMB, an important evaporation source during the August 2002 episode, behaves like a holding tank during summer: the vapor, together with pollutants, can accumulate for several days in a quasi-closed horizontal circulation, which results in a vertical pile-up of accumulation layers after coastal convergence, followed by return flows into the basin after divergence over the top of the coastal mountains. Vapor and pollution accumulation will continue for several days until a disturbance vents them off, ahead of the frontal system entering the area. Morning-to-evening cycles are inhibited before a new cycle of accumulation starts over the WMB. A similar process occurs in northern Africa around the Atlas Mountains [*Gangoiti et al.*, 2006a]: the convergence that takes place at the N-African thermal low will accumulate in the N-African mid-troposphere the pollutants and water vapor available at the Atlantic and Mediterranean marine boundary layers (MBLs). In addition, we showed that soil dust also accumulates in these layers [*Gangoiti et al.*, 2006a], which are mainly fed by daytime upslope flows in the southern flanks. These reservoir layers can move around the Atlas Mountains following the induced circulation of the N-African anticyclone. The moisture advection associated with transiting cyclones and fronts across the WMB, with a typical recurring time of about 3–10 days [*Millán*, 2007], can be increased by the above mechanism, if the cyclone phase and the proper dynamical forcing are simultaneously present. Therefore, the formation of moisture reservoirs could increase the likelihood of anomalous precipitation.

[5] This study aims at clarifying the role played by reservoir layers over the WMB in the extreme precipitation events of the 11–13 August 2002. Other marine evaporative sources like the Black Sea and the Eastern Mediterranean will also be investigated in order to clarify their contribution. We will need to track air masses with trajectories ending at a selected target area during the intense precipitation period (August 11–13, 2002) using a methodology that guarantees an accurate estimation of winds and stability at high resolution in an area of complex terrain like southern and central Europe. In this respect, the manuscript is organized as follows: the synoptic scenario during the precipitation episode in central Europe is described in section 2. Section 3 is devoted to the mesoscale simulation and its validation. The air mass tracing and the sequence of events during the episode is shown in section 4, as well as the discussion on the origin of the different air masses converging over the target area. Finally, in section 5 we summarize the main results. In a subsequent companion paper [*Gangoiti et al.*, 2011] we describe a new method developed by our group at the University of the Basque Country and the Fundación CEAM for identifying moisture source regions and quantifying their respective contribution to a selected target precipitation: the rainfall episode of August 11–13 is used for this application.

2. The Precipitation Episode: Synoptic Scenario

[6] During the first two weeks of August 2002, tracks of midlatitude lows were shifted south of their average location for this time of the year in southern Europe [*James et al.*, 2004]. During nighttime from August 5 to 6, a low formed between the Gulf of Genoa and the Alps. It moved eastward across northern Italy and the Adriatic Sea toward the Western Balkans, out of the WMB, leaving important rainfalls in central Europe on August 6–7 [*Ulbrich et al.*, 2003b]. On the following days, normal conditions over the WMB, with relative high pressures from August 6 to 9, favored coastal convergence and sea-breezes with the corresponding accumulation of pollutants (and moisture), as described by *Millán et al.* [1992, 1996, 1997] and *Gangoiti et al.* [2001, 2006a].

[7] The accumulation mode ceased abruptly during the passage of a new disturbance: the cyclone *Ilse*, located over southern England on August 9, intensified over the Gulf of Genoa on August 10. The cyclone inhibited the coastal convergence of sea-breezes and the compensatory subsidence over the western basin, and forced intense southwesterlies into the region. This resulted in warm and moist air advection at lower levels, which crossed the Italian peninsula, the Adriatic Sea and the western Balkans into central Europe, along a cyclonically curved path. During August 10 and until 0000 UTC on August 11, the track of the surface low *Ilse* moved slowly across northern Italy into the Adriatic Sea [*Ulbrich et al.*, 2003b]. At upper levels, the 200 hPa flow showed a trough in the jet stream associated with the formation of *Ilse* on August 9 (not shown). On the next day, the trough moved southward and intensified first over the Gulf of Lyon and then over the Gulf of Genoa during August 11, showing a very tight short wave at 1200 UTC (Figure 1d) with a 50 ms^{-1} jet streak, unusual for the summer: the upper level divergence produced over central Europe is depicted in the same panel (white dashed line), which shows a large area of negative pressure vertical velocities (ascending air). Figure 1 also shows the 500 hPa geopotential height and relative vorticity, the 850 hPa winds, temperature and moisture, and the sea level pressure with the 1000–500 hPa thickness. The area with the lowest surface pressures in central Europe corresponds to the upper

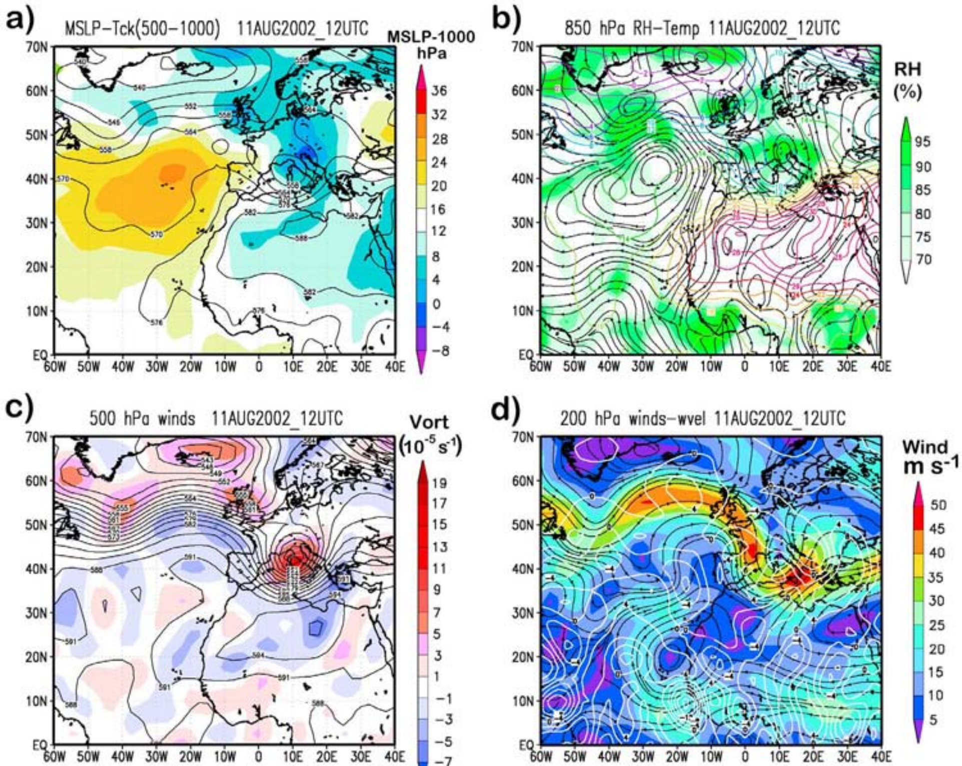

Figure 1. NCEP-reanalysis at 1200 UTC on August 11: (a) mean sea level pressure MSLP-1000 (hPa) in shaded colors and 1000–500 hPa thickness (dam) in contour lines; (b) 850 hPa streamlines, relative humidity (%) and temperature (°C) in colored contour lines; (c) 500 hPa geopotential heights (dam) with the relative vorticity (1×10^{-5} s^{-1}) shaded; and (d) 200 hPa winds (streamlines and magnitude in shaded colors) with the pressure vertical velocity (1×10^{-2} Pa s^{-1}).

level divergence and air ascending in the whole depth of the troposphere (Figure 2). The tracing of air masses, which will be discussed in section 4 after the mesoscale simulation, will show that the warm air located over the western and central Mediterranean before August 10 was running ahead of the trough in a highly curved trajectory on August 11 (temperatures above 12–14°C in Figure 1b and thickness above 564 dam in Figure 1a). The region between latitudes 45–50 N, located to the north of the vorticity maxima, shows ascending air with high relative humidity (Figure 2): it corresponds to the region of extreme precipitation, and it is located at the boundary between the cold north-Atlantic advection to the south and the warmer Mediterranean air to the north.

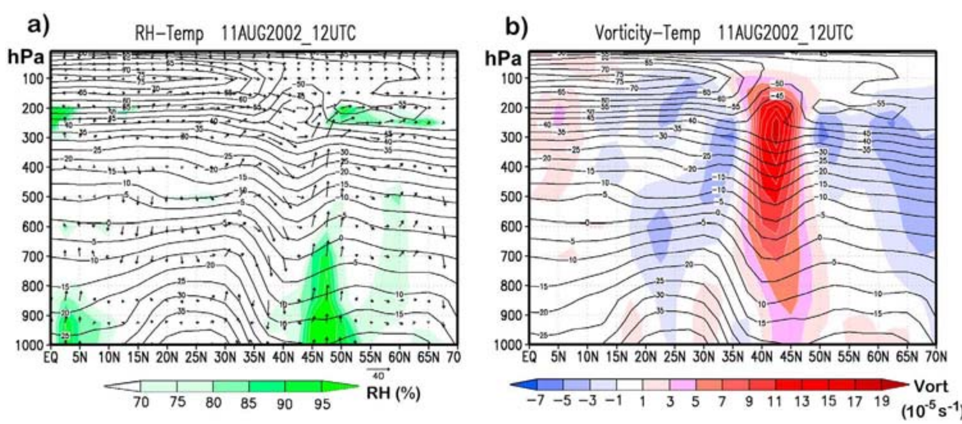

Figure 2. Vertical cross section across the shortwave observed in Figure 1 (longitude 12.5 E), showing (a) relative humidity (%) in shaded colors, temperature (°C) in contour lines and winds, depicted with the meridional and vertical component (v, pressure vertical velocity -1×10^{-2} Pa s^{-1}) and (b) relative vorticity (1×10^{-5} s^{-1}) together with temperature (°C) in contours.

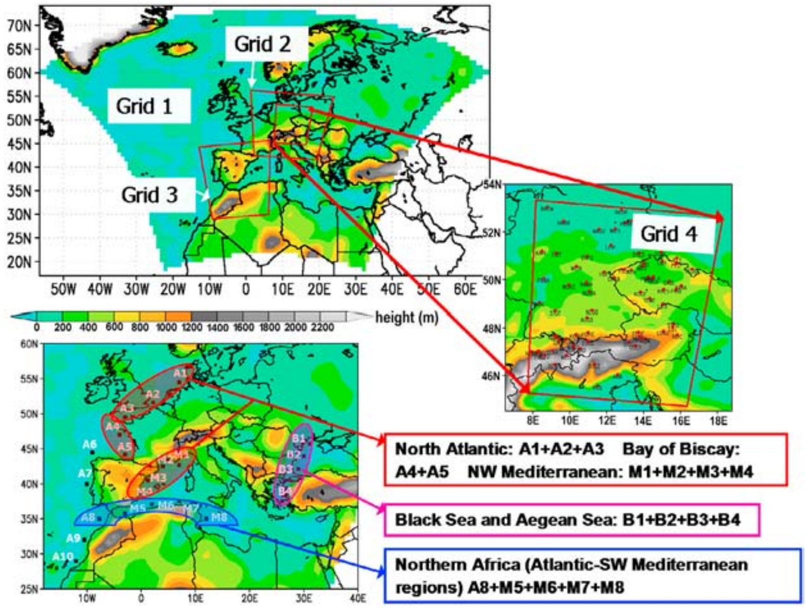

Figure 3. Topography and coverage of domains for the RAMS-HYPACT modeling system. Grid 4 is approximately coincident with the target area of precipitation and has the highest resolution. This zone is now the Czech Republic, Germany, Austria, Switzerland and Italy and also Slovenia and Croatia (in the southeast corner of grid 4), which are not represented within the area of the former Yugoslavia (the current political borders have not been updated). The position of the HYPACT tracer sources are represented in the lower-left panel.

[8] In the early morning of August 12 the surface trough reached its lowest pressure over central Europe (the Czech Republic), after turning northward from the Adriatic Sea, and started to leave the area, advancing eastward fairly slowly. The target area, which received the highest precipitation amounts during the August 11–13 episode, was finally a vast region comprised between 45 and 53 N latitude and 8–16 E longitude; it will be marked with a square in the tracing experiments performed in section 4.

3. High-Resolution Simulations and Mesoscale Model Validation

[9] The combined application of the Regional Atmospheric Modeling System (RAMS) [*Pielke et al.*, 1992] and the HYbrid PArticle Concentration and Transport model (HYPACT) [*Tremback et al.*, 1993], and an adequate selection of domains/resolutions have allowed us to explain episodes of long-range transport of ozone in northern Iberia and the WMB [*Gangoiti et al.*, 2001, 2006b], and the mechanism for the accumulation and transport of Saharan soil dust and pollution from southern Europe to the tropical Atlantic and the Caribbean [*Gangoiti et al.*, 2006a]. Using this methodology, tracks from continuous emissions of selected sources can be used to detect preferred pathways, travel time(s), accumulation layers and the convergence and venting mechanisms of these air masses.

[10] A similar method is applied here, using the most recent version of the modeling system RAMS (v6.0) and HYPACT (v1.5) along with new domain coverage and resolutions to cope with the objective of adequately simulating the transport of vapor from source areas into the target area. A good representation of the precipitation over the region and a good synchronism of events between observations and simulations are required to be confident with the HYPACT results, which will simulate trajectories for several days. The topography and coverage of the four selected domains (two-way nested grids) of the RAMS-HYPACT modeling system are presented in Figure 3. Grid #4 is approximately coincident with the precipitation target area, and it has a resolution of 9 km. Intermediate grids #2 and #3 have a resolution of 27 km, and the lowest resolution (108 km) corresponds to grid #1. The vertical coverage of all grids is 22 km, with maximum resolution at lower levels (30 m) decreasing to a minimum of 1000 m above the 11 km height. Four-dimensional data assimilation was used for the model run, with Newtonian relaxation toward the 6-hourly NCEP reanalysis data [*Kanamitsu et al.*, 2002]: a variable relaxation time was used, with the highest values (weak nudging) at the center of the large domain (grid #1) and lowest values (strong nudging) at the boundaries. The run of the mesoscale model performed continuously, from July 27 through August 16, 2002. The topography and land cover were interpolated from the USGS global 30″ database [*Gesch et al.*, 1999; *Anderson et al.*, 1976]. Weekly averages of the sea surface temperature (SST) data, with a resolution of 1° × 1°, were interpolated from the NCEP Reynolds SST data set [*Reynolds and Smith*, 1994]. As the model run extended for more than one week, SST values were interpolated in time during the model run. Our setup included a prognostic turbulent kinetic energy (level 2.5) parameterization [*Mellor and Yamada*, 1982], with modifications for a case of growing turbulence [*Helfand and Labraga*, 1988], and a full-column two-stream parameterization that accounts for each form of condensate (7 species) for the calculations of the radiative transfer [*Harrington*

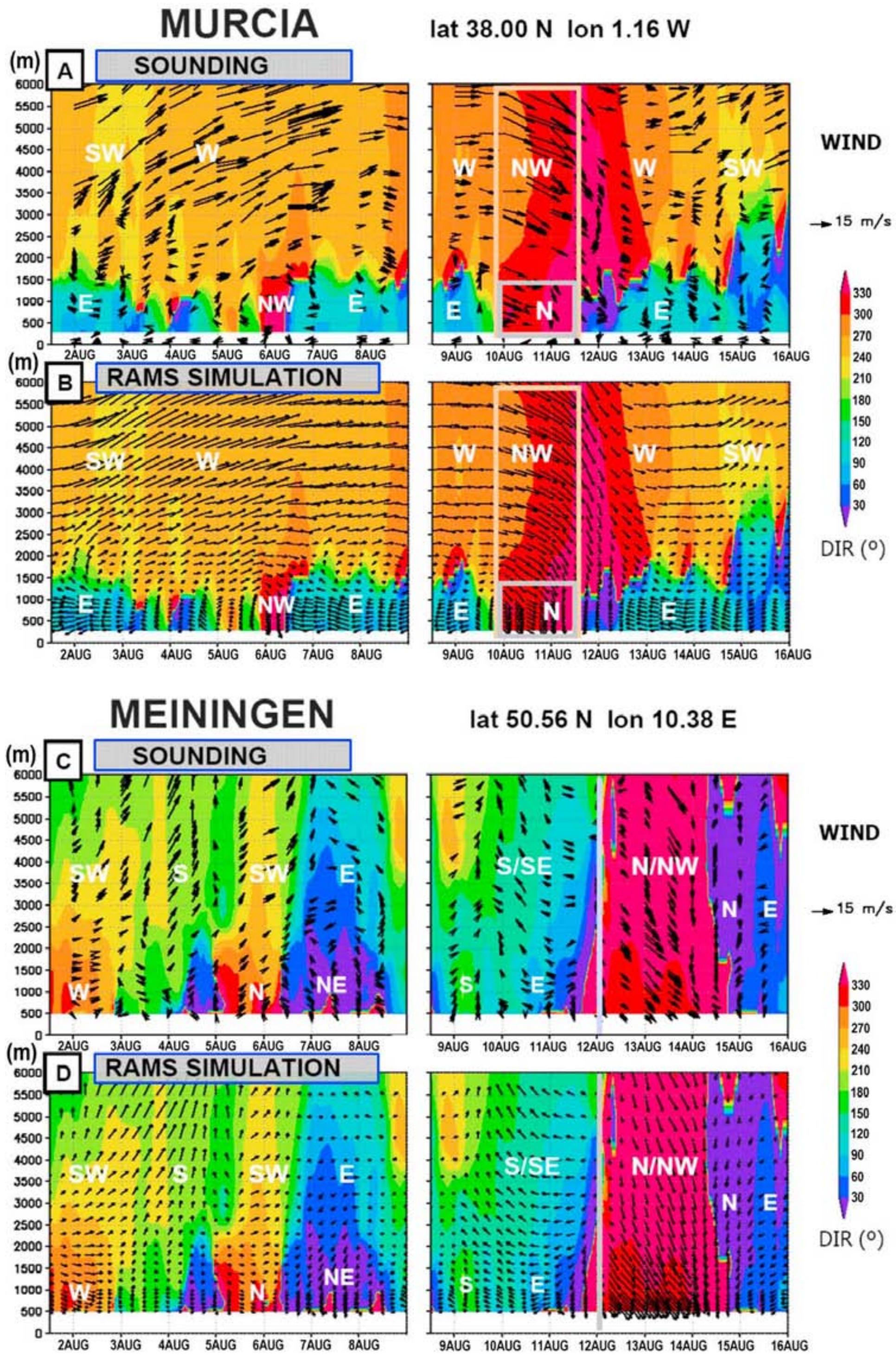

Figure 4. (a, c) Observed and (b, d) simulated wind profiles at Murcia (Figures 4a and 4b) and Meiningen (Figures 4c and 4d) from August 2 to August 16.

et al., 1999]. The cloud and precipitation scheme by *Walko et al.* [1995] was applied in all the domains with all the species activated, and the LEAF-3 soil vegetation scheme was used to calculate sensible and latent heat flux exchanges with the atmosphere, using prognostic equations for soil moisture and temperature [*Walko et al.*, 2000]. After the mesoscale meteorology simulation, hourly wind and turbulence fields obtained by RAMS were fed to the HYPACT model to track the water vapor from a selection of sources.

[11] Figure 3 shows the position of the tracer sources, comprising a total of 22 vertical emission line sources, from surface level to 500 m height, placed at the main entrances of marine water vapor to continental areas: WMB (M1 to M8), the Atlantic Ocean (A1 to A10) and the Black Sea

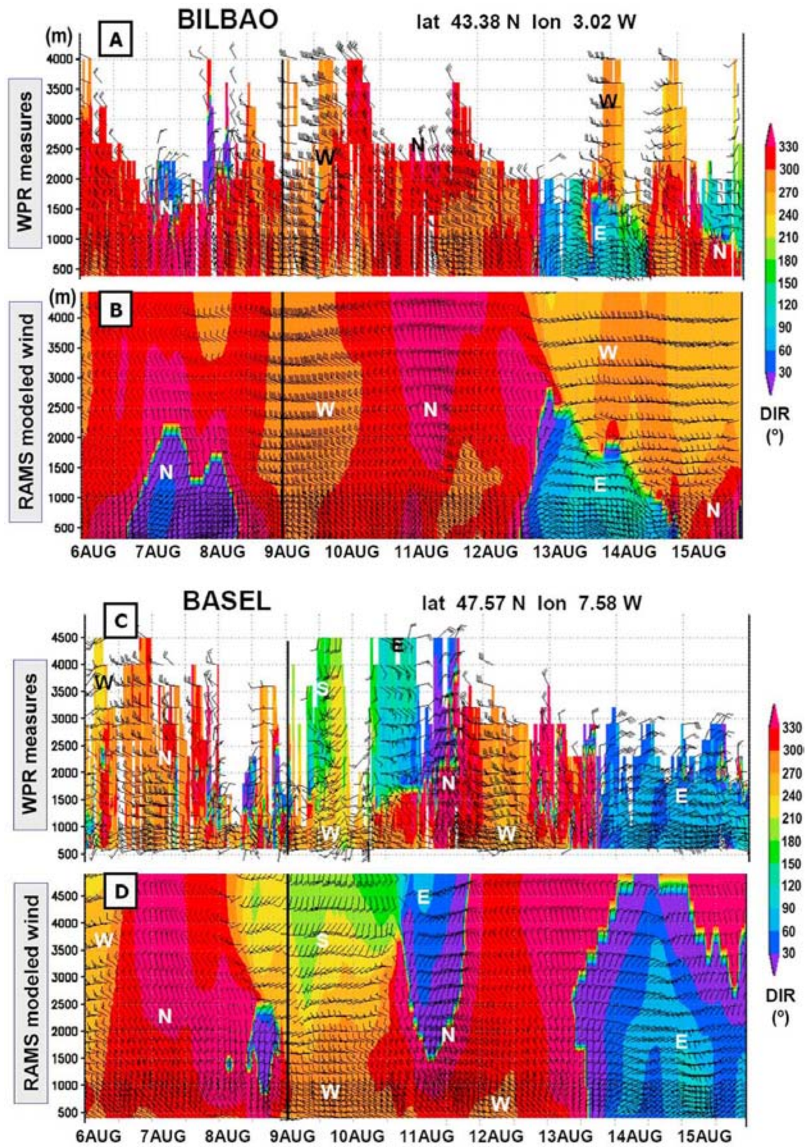

Figure 5. Time sequence (August 6–August 15) of the (a, c) observed and (b, d) simulated wind profiles on the vertical of two wind profiler sites: Bilbao (Figures 5a and 5b) and Basel (Figures 5c and 5d). The wind direction is depicted in shaded colors.

together with the Aegean Sea (B1 to B4). The 5 marked regions in Figure 3 are used to show their respective contribution as 'area sources' by adding the tracer particles emitted from them. Consequently, only air masses with an initial marine origin are tracked and the role of the terrestrial evaporative sources is discussed in the second part of this paper [*Gangoiti et al.*, 2011]. A total of 85200 particles per source were released continuously from July 27 to August 14, and particle locations were tracked for the whole period of simulation (20 days) without being removed by any other mechanism but the venting out of the largest domain boundaries of grid 1 in Figure 3.

[12] The described setup of the modeling system was chosen after having discarded other alternatives, with a different number of grids, domain coverage, resolution, and type of nudging. After every trial, we validated the RAMS meteorological output with NCEP data, wind and temperature profiles from the European NMC stations, output from wind profiler radars (WPR) in Bilbao and Basel, surface precipitation at the target area, MODIS total precipitable water vapor, and precipitation data from the TRMM MultiSatellite Precipitation Analysis (TMPA). Results shown here were found to be the best representation of the mentioned set of observations.

[13] The hourly wind speed and direction calculated by the model and the experimental measurements from two radiosonde stations and two WPRs are represented in Figures 4 and 5. These are located near the Atlantic and Mediterranean moisture sources (Bilbao and Murcia) and inside the target rainfall area (Basel and Meiningen). The simulated and observed wind profiles agree satisfactorily: the high-resolution simulation was able to capture both the intensity and the timing of the coastal sea-breezes and drainage winds recorded in Murcia and the suppression of

Table 1. Wind Comparisons Between WPR Observations and RAMS Evaluations[a]

	Bilbao	Basel
BIAS u	−1.14	1.05
BIAS v	−0.42	−1.84
RMSVE	3.47	4.88
RMSE u	2.68	3.03
RMSE v	1.66	3.20
Correlation u	0.74	0.73
Correlation v	0.82	0.63

[a]Statistical comparison between the observations from two wind profiler radars located in Bilbao and Basel, and wind evaluations by the mesoscale model RAMS.

these mesoscale flow regimens coincident with the passage of *Ilse* on August 10–11 (marked with a gray square), as well as the change from southerly to northwesterly winds observed in Meiningen on August 12 (indicated with a gray line). The same can be concluded from the comparison of the modeled wind profiles with the WPR outputs at Bilbao and Basel (Figure 5). The statistical values (BIAS, RMSVE, RMSE and correlation, defined by *Zhong and Fast* [2003], summarized in Table 1, confirm the good agreement between experimental measurements and simulations: despite a slight general underestimation, our RAMS set-up was able to simulate wind profiles with statistical scores comparable to those of other similar studies [*Hanna and Yang*, 2001; *Zhong and Fast*, 2003].

[14] Precipitation totals during the episode (August 11–13) are shown in Figure 6: the distribution of the simulated precipitation (left panel) and the surface station data (right), as depicted by *Rudolf and Rapp* [2003], cover a similar region with an identical maxima-minima distribution. Regions with maxima above 180 mm are observed in both panels of Figure 6 as well as in the TMPA data (not shown). Outside of this region, with lower grid-cell resolutions, the precipitation was underestimated by RAMS, while the coverage of the areas with precipitation was well estimated. As a consequence, it seems that we need at least a grid-cell resolution similar to that used in grid #4 to obtain an accurate precipitation estimate in all regions.

[15] Evolution of the water vapor total column is represented in Figure 7 for August 9 to 12, as shown by MODIS-TERRA IR images (left panels) and RAMS model simulations (right panels). MODIS images have a resolution of 1 × 1 degree and areas covered by clouds (in white color) contain no vapor data. Venting of the vapor over the Mediterranean to the E and NE, ahead of the disturbance, is synchronous in both sets of panels. The main differences in vapor totals are concentrated in the lower left corner of the figures, at the SW boundary of grid #1, where vapor from the African Inter Tropical Convergence Zone (ITCZ) breaks out into the Atlantic. Above latitude 25 N and over the landmass of northern Africa most of the vapor is accumulated in the middle troposphere (700–300 hPa), which is really an outstanding feature: Figure 8a (left) shows this important concentration of water vapor observed by MODIS. When compared with the total column in the top panel of Figure 7 (color scale is kept constant in both figures), it can be observed that practically all the vapor in N-Africa is at that height range (700–300 hPa), and that its column, at regions with high values (1.5–2.0 cm), is close to one half of the total column maxima found over the Mediterranean Sea (4.0–5.0 cm in Figure 7, left). Thus, the water vapor mixing ratio over the northern Africa landmass shows an anomalous vertical distribution, with the lowest values at the surface, increasing with height, and the highest values in the middle troposphere. This anomalous pattern is the result of the same meteorological mechanism responsible for the accumulation of dust around the Atlas Mountains: for water vapor, it applies to the convergence and recirculation of moisture vented to the middle troposphere by the combined

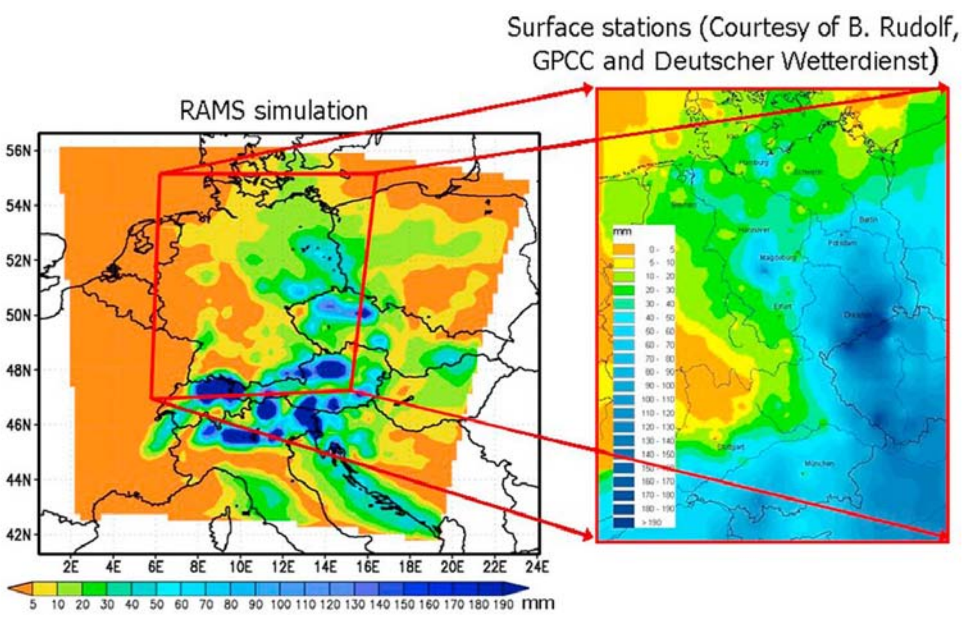

Figure 6. Distribution of (left) simulated precipitation and (right) surface station data, as depicted by *Rudolf and Rapp* [2003]: totals from 06 UTC August 10 to 06 UTC August 13.

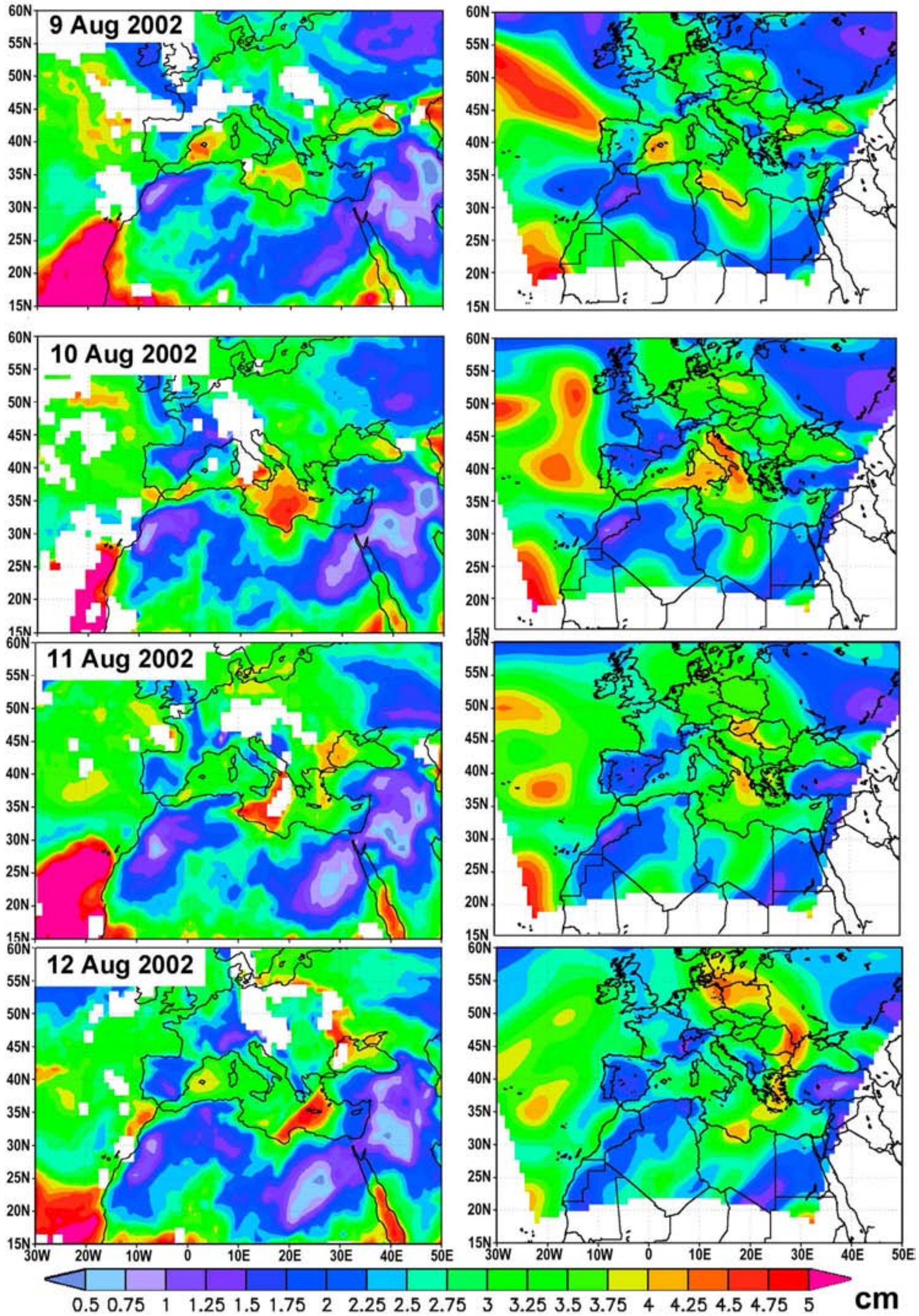

Figure 7. Evolution of the water vapor total column from August 9 to 12, as shown by (left) MODIS-TERRA IR images and (right) RAMS model simulations.

upslope flows and coastal sea-breezes around the Atlas Mountains, as described in section 1.

[16] Because the mesoscale model has demonstrated its ability to successfully simulate the observed winds, transport of moisture and precipitation in the target region of central Europe, we will now merge the modeled data and the observations in Figure 8 to show the accumulation processes around the Atlas Mountains and over the WMB during the period August 6–9: Figures 8a (top) and 8b (top) depict the moisture and winds on August 6, while Figures 8a (bottom) and 8b (bottom) show the same data for August 9. August 6 corresponds to the initiation of the WMB accumulation mode after the passage of cyclones over the area. It should be mentioned that, at the same time (August 6–7), large areas of central Europe, northern Italy, and the Western Balkans recorded torrential rains, which contributed to significantly raise water levels in several small rivers of Lower Austria, and also to raise soil saturation levels in the catchment areas of both the Elbe and Danube rivers (section 2). In contrast, August 9 corresponds to the ending

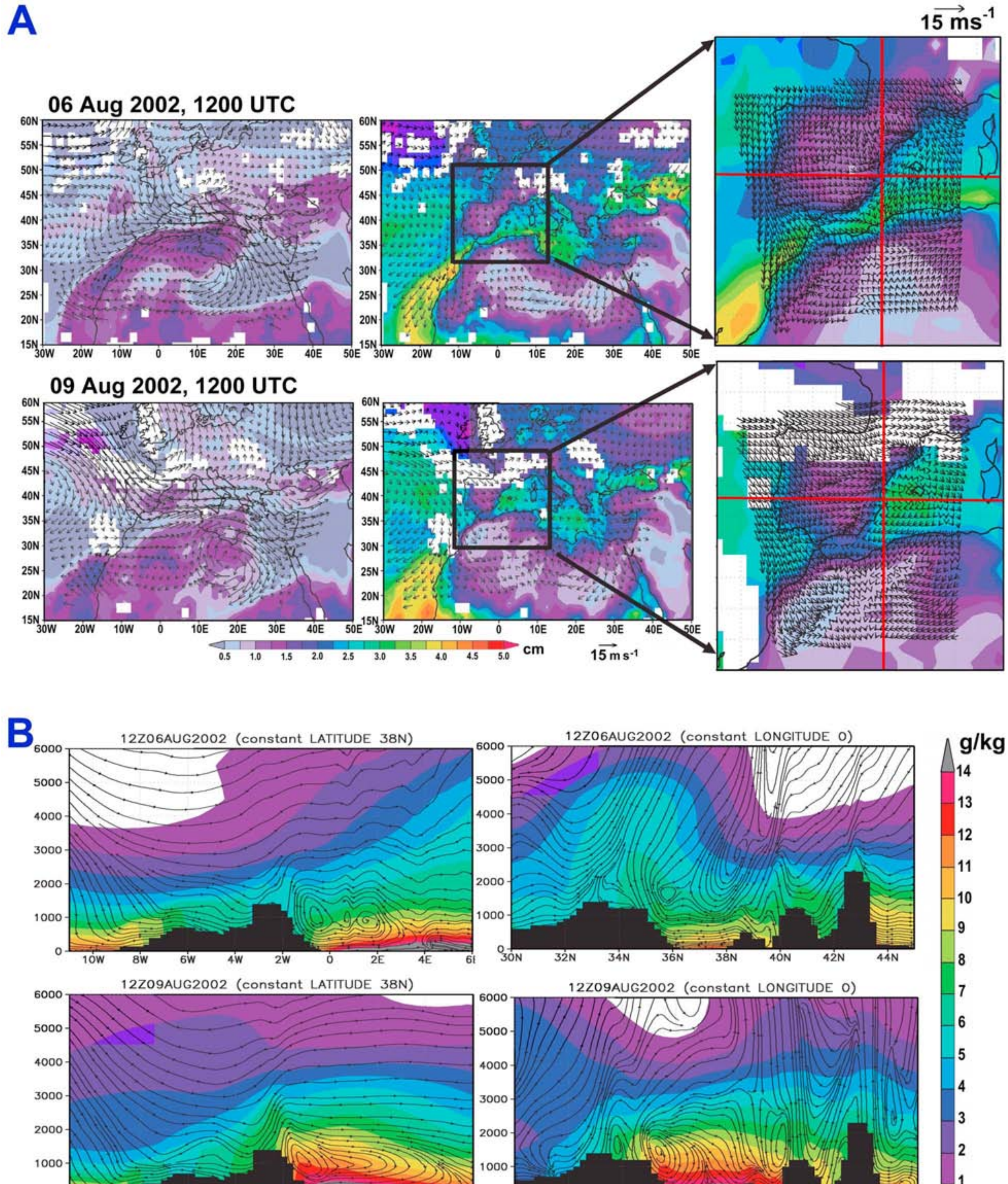

Figure 8. Vapor distribution during the first (August 6) and last (August 9) day of the accumulation period in the WMB: (a, top left) MODIS water vapor column between 700 and 300 hPa, together with simulated winds (grid #1) transporting the vapor (winds at 3600 m above ground); (a, top middle) MODIS water vapor column from ground level up to 700 hPa together with winds at ground level; (a, top right) Enlarged view of the MODIS lower water column, together with surface wind simulations at grid #3 (higher spatial resolution); (b, top left) vertical cross sections of the simulated vapor mixing ratio with u-w streamlines at constant latitude 38 N, and (b, top right) cross section at constant longitude 0 and at 1200 UTC August 6.Terrain profile is represented in black at the bottom. Figures 8a (bottom) and 8b (bottom) show a similar set of drawings for August 9.

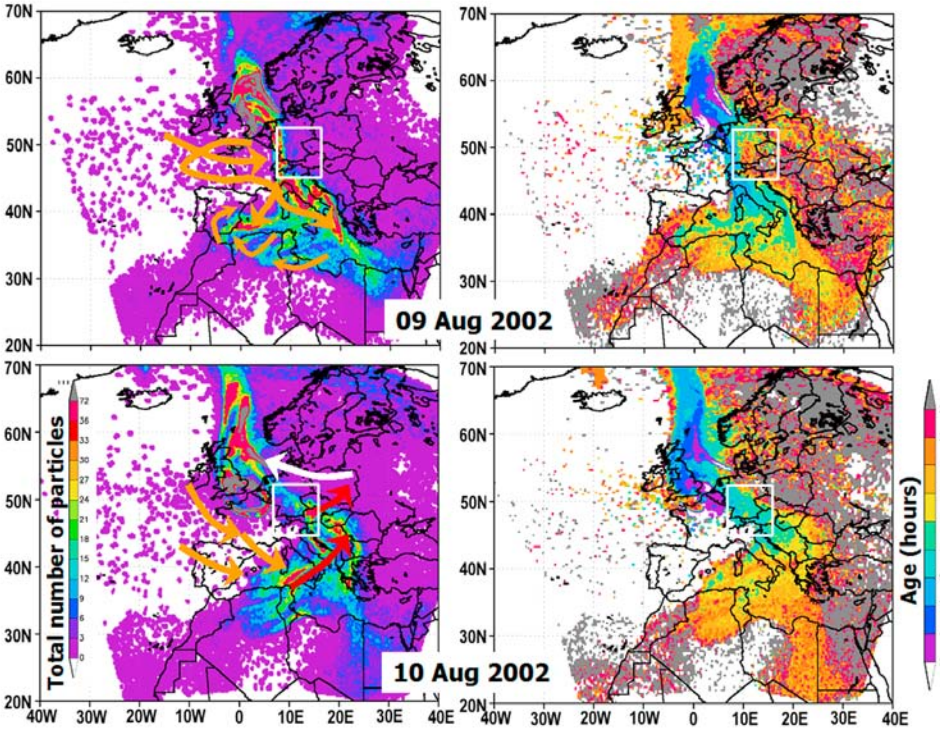

Figure 9. Tracks of the N-Atlantic tracer (total number of particles) (top left) at the end of the accumulation period in the WMB on August 9 and (bottom left) after the irruption of cyclone Ilse, and (right) age of the respective tracks. The disturbance vented the accumulated vapor out into the target area (white square): red arrows in the lower-left panel indicate that the tracer is vented to the middle and upper troposphere, ahead of the frontal system. Rainfall maxima in central Europe occurred on the following days: August 11 and 12.

of the accumulation mode. During this 4-day period, the coastal convergence (sea breezes-upslope flows) and sinking over the WMB accumulated vapor over the reservoir layers of the basin, following the aforementioned scheme by *Millán et al.* [1997], while convergence around the Atlas Mountains fed the middle troposphere reservoir over northern Africa. The mechanisms behind this accumulation are illustrated in the vertical cross sections of the simulated water vapor mixing ratio (shaded colors) and the cross wind components (u-w and v-w streamlines) at a constant latitude 38 N (Figure 8b, left) and at a constant longitude 0 (Figure 8b, right) during these two days (August 6 and 9, 12 UTC). The cross sections show the deep vertical injections that take place both over eastern Iberia (3000 m) and over northern Africa (>5000 m) as a result of the combined sea-breeze and upslope daytime convergence over the coastal range of mountains. These injections, and their return flows back over the sea, lead to the vertical recirculation of the water vapor and to its accumulation over the WMB (see changes in the water column from Figure 8a (top middle) to 8a (bottom middle), as well as from Figure 8b (top left) to 8b (bottom left) and Figure 8b (top right) to 8b (bottom right)), while another fraction is transported within the anticyclonic gyre of the N-African mid-tropospheric circulation. The layer containing more than 4 g/kg of water vapor extends up to 3000–4000 m over eastern Iberia and northern Africa on August 9. On August 10 (Figure 7), the effects of the passage of the Atlantic cyclone *Ilse* over the WMB are clearly observed: the sea-breeze convergence over the crest of the mountains is inhibited, and the frontal system vents off the water vapor into central and eastern Europe, reducing the total column of water vapor over the western Mediterranean from 3.75 to 4.0 to 1.75 cm in less than 12 h.

4. Tracing of Air Masses and Discussion

[17] Two issues must now be addressed: the source of the water vapor responsible for the central Europe precipitation events on August 11–13, and the role of the WMB and N-African vapor accumulation layers in the precipitation on the target area. On August 9, 2002, the accumulation period over the WMB, initiated on August 6 after the massive intrusion of an air mass of N-Atlantic origin through southern France and the Gulf of Lyon, entered its last day. This period is observed in Figures 4a and 4b, at the coastal station of the WMB (Murcia), between the initiation and finishing of the easterlies regime (sea-breeze regimes at eastern Iberia) flowing at lower levels and decoupled from the westerlies blowing on top. The frontal irruption is always followed by intense northerlies (colored in red in the figure), which blow after a short period of southerlies (colored in green). Notice that this systematic decoupling is not observed in the Meiningen station. The left panels in Figure 9 show the track of the tracer emitted in the N-Atlantic region (total burden of tracer particles), while the right panels show the age of the tracked particles (each color corresponds to a time lapse of 24 h). August 9 and 10 (1200 UTC) correspond to the end of the accumulation period over the WMB and the

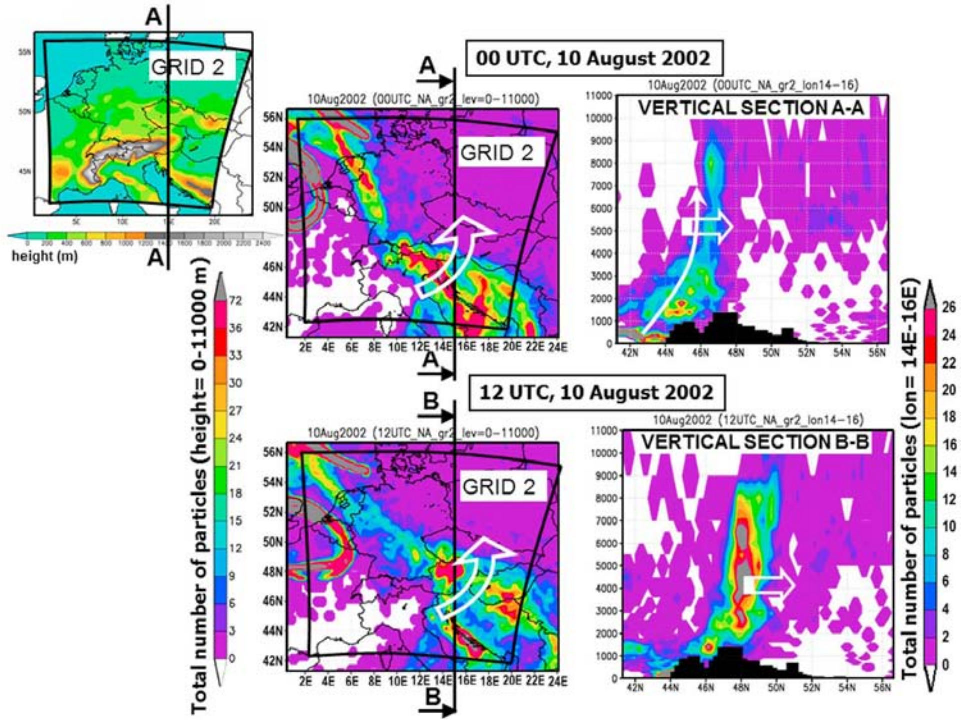

Figure 10. (middle) Plan views and (right) vertical sections of the N-Atlantic track when approaching the target area on August 10. The plan view is shown using an amplified window (grid 2) of the region represented in Figure 9 (bottom). Vertical venting over the Western Balkans and horizontal transport around the Alps in a curved trajectory (white arrows) are shown. (left) The topography of the region; its vertical section, at longitude 15E, is colored in black (in the right panels).

initiation of the transport into central Europe under the perturbed conditions created in the region by cyclone *Ilse*. Arrows show the wind transporting the main fraction of the tracer: on the upper-left panel they show the main paths into the Mediterranean. Once inside the basin, the western branch follows the combined upslope flows and coastal sea-breezes of eastern Iberia and northern Africa during the accumulation period of August 6 to 9, while the eastern branch drifts slowly southward, parallel to the Italian Peninsula, from August 7 to 9. Following our simulations, the main fraction of the tracer was transported over the Mediterranean Sea in the lower troposphere (0–2000 m). For the lower 1000 m, the water vapor entered the Mediterranean with an average mixing ratio of 8.5 g/kg and exited with 12.5 g/kg, after being transported (following the irruption of Vb cyclone *Ilse*) through the Italian Peninsula and the Adriatic Sea. Then, it crossed the Western Balkans and Eastern Europe into the target area during August 10 (Figure 9, bottom): red arrows indicate that the N-Atlantic tracer was vented to the middle and upper troposphere. The low level flow forced by the Scandinavian Anticyclone, ahead of the disturbance, is marked with a white arrow in Figure 9.

[18] Similar tracks are observed for the tracer emitted from the Bay of Biscay and from the WMB itself (not shown). The massive intrusion into the WMB for the tracer released at the Bay of Biscay also occurred on August 6 through the Gulf of Lyon. A smaller fraction crossed Iberia over the Ebro Valley into the WMB. The main differences with the N-Atlantic tracer are related to the time of arrival at the target area on August 11. As mentioned in the previous paragraph, the main fraction of the joint tracer released from all these sources (marked in red in Figure 3) was vented to the middle and upper troposphere (0–8000m) before arriving at the latitudes of the target area: Figure 10 shows a detail of the venting of the N-Atlantic tracer over the Western Balkans at 00 UTC and 12 UTC on August 10. The figure also shows the topography of the region as well as a plan view and vertical cross-section of the tracer distribution. The joint air masses warmed and moistened in the WMB entrained additional water from evapo-transpiration over the Western Balkans, increasing their mixing ratio before arriving at the target area on August 11. However, our mesoscale model results show that the precipitation during the trajectory over the Balkans would probably have compensated the evapo-transpiration, since the water vapor total column remained constant within the air mass (4 cm), and the average vapor mixing ratio of the lower 1000 m kept at the same values as when leaving the Adriatic Sea (12.5 g/kg).

[19] Figure 11 shows the time-sequence of the daily evaporation (accumulated during each 24 h) attributed to the initial precipitation (0000–1200 UTC, August 11) in a southern subset of the target rainfall area (named SR in the companion paper), which includes Upper Austria and southeastern Germany. The heavy rain started and ended somewhat earlier in this region than in the north and northeast (named NR). Most of the observed evaporation areas, estimated by the new methodology presented in the companion paper, follow the surface trajectories of the winds transporting the air mass entering the WMB during the accumulation period. Since the main fraction of the attribution occurs during the 6-to-8 days

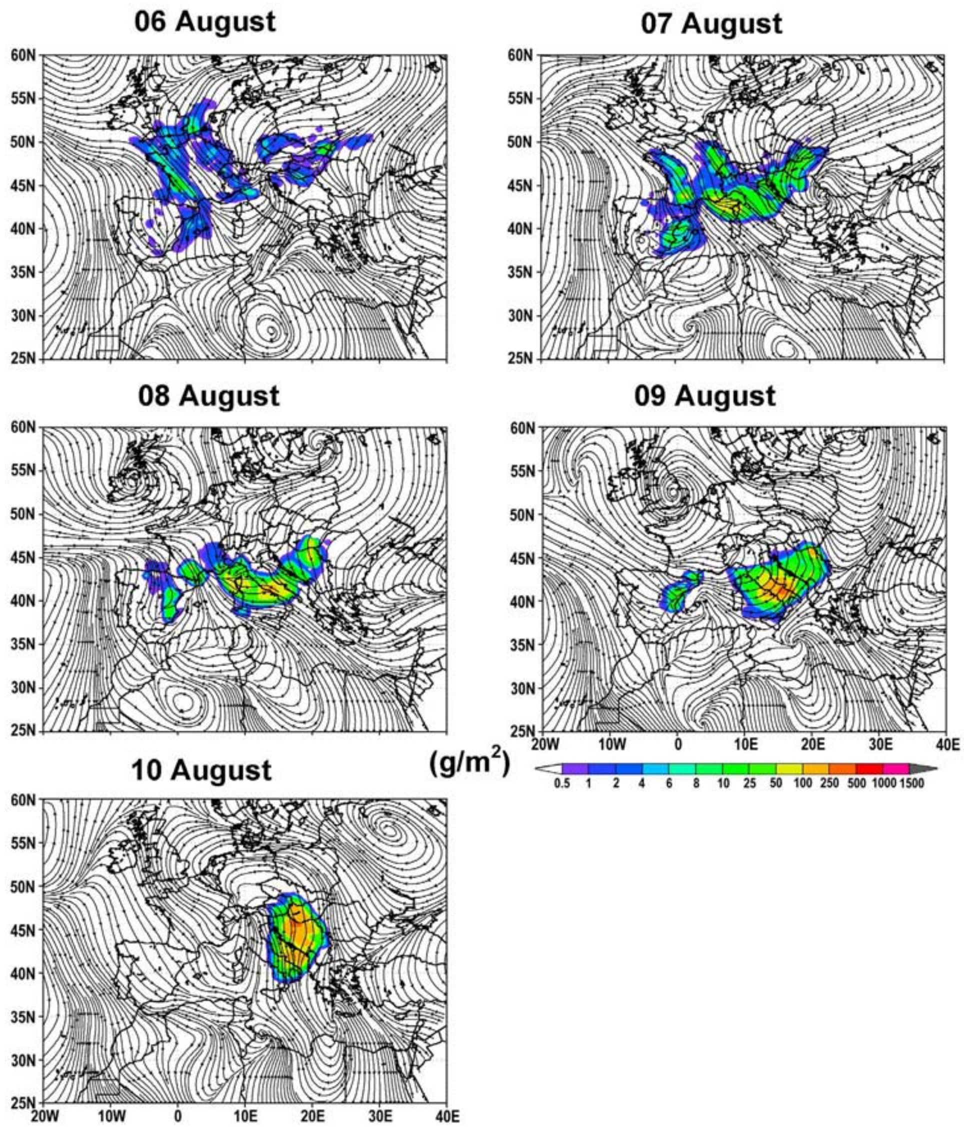

Figure 11. Sequence of daily evaporation maps during the accumulation period (6–9 August) and during the convergence into the central Europe target area (August 10), attributed to the initiation of the precipitation episode (0000–1200 UTC, August 11) in a southern subset of the main rainfall area (12–15E, 47.5–48.5 N). The simulated surface streamlines at midday are also represented.

preceding the precipitation event, as is shown in the companion paper, the Figure 11 represents main moisture sources during the initiation of the event in the southern region of the target rainfall area. The evaporation at the eastern and western branches of the air masses entering the WMB is observed in the figure from August 6 to 9, while on August 10, the evaporation is centered inside the trajectories approaching the target, including the Adriatic Sea and the western Balkans.

[20] Figure 12 (top left) shows how the tracer entered the target area on August 11, after crossing the Balkans and Eastern Europe and veering to the West pointing to the low pressure region developed at the northern flanks of the Alps during the evolution of cyclone *Ilse*. As shown in the upper-right panel, the age of the tracer is 168 h (7 days): it was emitted on August 4 from the N-Atlantic region (Figure 3) and, after a long journey across the WMB, moved to the North again. The tracer reached the latitudes of the target area not so far from the region where it was released 7 days before, at that time flowing within a colder and drier air mass. There is a clear similitude between the position of the curved track of the tracer around the target and the area with high relative humidity at the 850 hPa level, depicted in Figure 1. On August 11, while the tracer moved to the West, parallel to the northern flanks of the Alps, intense precipitations were recorded over the target region, and the pressure decreased to its minimum values. Figure 12 (middle and bottom) shows how cool N-Atlantic air moved across northern France on August 12 and 13, in a direct NW-to-SE trajectory toward the target area, and encountered the old, moist, and warmer air mass located over the region. The frontal system formed by the two air masses is better observed in the right panels, looking at the age of the tracer over the target area. Intense precipitations were also recorded in the region during August 12, lasting until the early morning

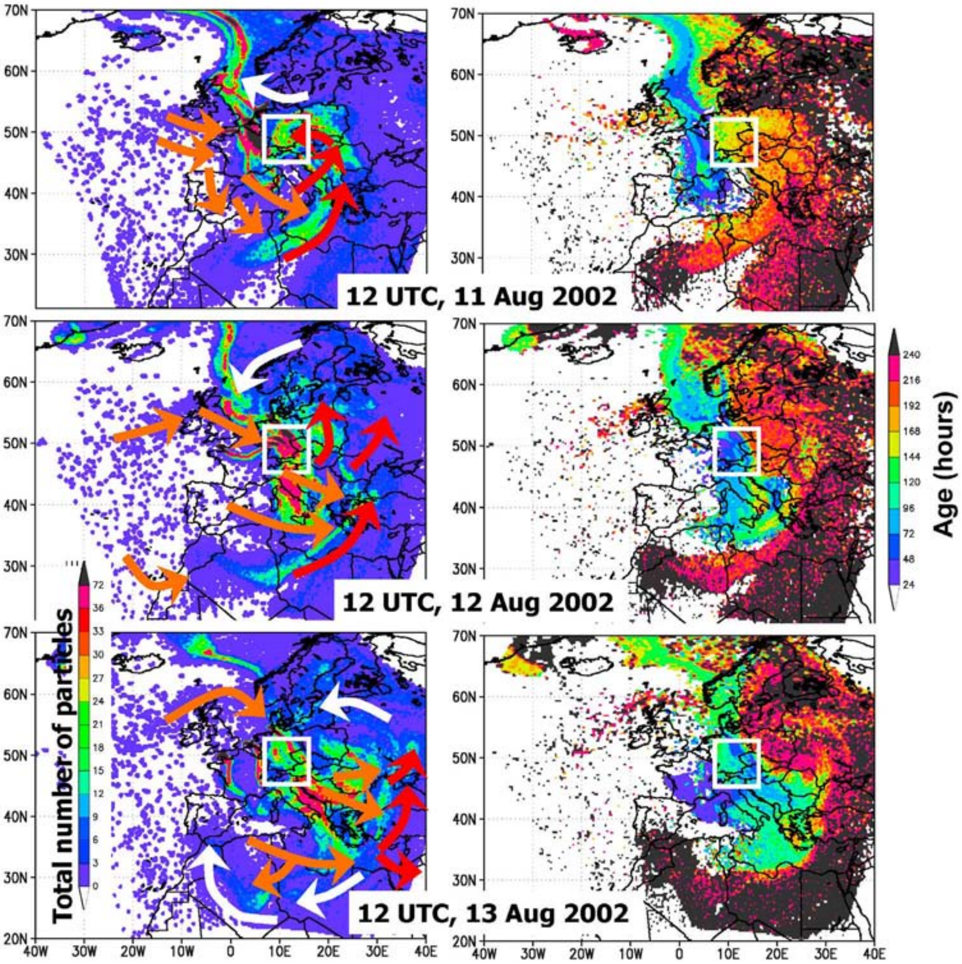

Figure 12. (left) Tracks of the N-Atlantic tracer during the rainfall maxima in central Europe from August 11 to 13, and (right) the age of the tracks. The tracer crossing the Balkans on August 10, moved westward into the target area on August 11 (in the top left panel). This aged tracer (in the right panels) encountered new tracer emissions with the same N-Atlantic origin traveling directly inland into the central Europe target region on August 12 (in the middle panels). At the same time, over southern Europe, the disturbance crossed the central Mediterranean and entered the Black Sea region. During the morning of August 13, the old tracer (transported across the WMB) was removed from central Europe (in the bottom right panel), and the precipitation decreased in the region and intensified over the Black Sea (from 12 UTC, August 12).

of August 13: the rainfall events moved into the E and NE region of the target area, following the slow movement of the frontal system.

[21] From 12 UTC August 12 until August 13 intense rain episodes were also observed in the western Black Sea region (Bulgaria, Romania and Ukraine), moving from the SW to the NE of the region, ahead of the frontal system located over the Mediterranean Sea and associated with cyclone *Ilse*. The frontal system is clearly discernible in Figure 12 (right middle and right bottom), with the blue colors facing the more reddish colors of the old tracer. Next, we will show that the air mass running ahead of the frontal system at the Black Sea contains a larger fraction of the N-African tracer, together with emissions from the Black Sea and the Aegean Sea.

[22] To investigate the role of the N-African accumulation layers, we have to track the trajectories of the tracer emitted from the blue colored region in Figure 3. As observed in Figure 13, the tracer does not penetrate deeply into the central Europe target area, but rather moves around the East and North boundaries of the region. However, during the severe rainfalls observed in the western Black Sea region (August 12–13), the N-African tracer can be observed running ahead of the frontal system crossing the eastern Mediterranean on August 12 (Figure 13, middle and bottom): the tracer, previously accumulated in the N-African middle troposphere, is now vented out with the southwesterlies over the western region of the Black Sea. The same panels in Figure 13 show the recovery of the normal/accumulation mode in the middle troposphere of N-Africa, initiated by the restitution of the upper flow behind the frontal system (white arrows), as described by *Gangoiti et al.* [2006a].

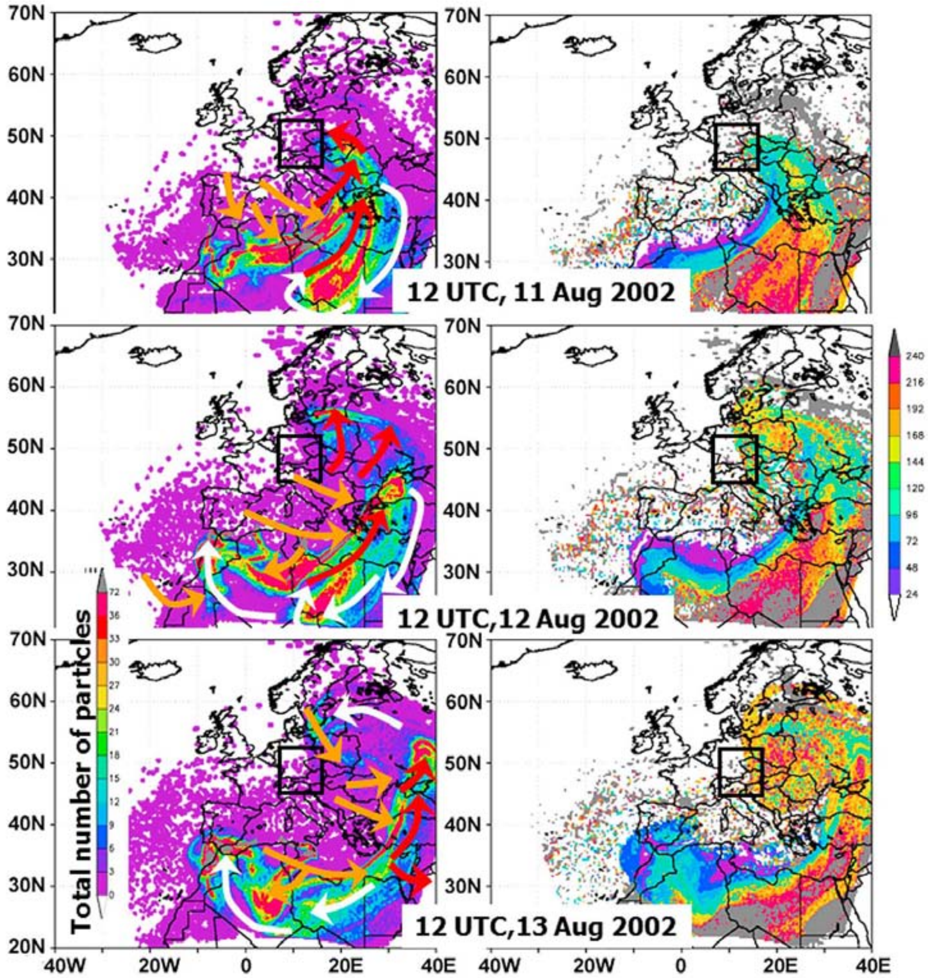

Figure 13. (left) Tracks of the N-African tracer during the rainfall maxima in central Europe from August 11 to 13, and (right) the age of the tracks. The main fraction of the N-African accumulation layers, following the tracer trajectories (red arrows), did not penetrate into the target area of central Europe (marked with a black square). The tracer moved along the East boundary of the region. However, during the second half of August 12 and during all August 13, intense rainfalls were registered in wide areas of the western Black Sea region (Bulgaria, Romania and Ukraine). These rainfalls do have a clear relationship with the N-African vapor accumulation layers, which as shown in the middle and lower panels, moved ahead of the frontal system marked by the tracks of the N-Atlantic tracer in Figure 12.

[23] According to our simulations, the air masses evaporated from the violet-colored region in Figure 3 (Black Sea and Aegean) did not contribute to the precipitation in central Europe during the first stage of the episode (Figure 14, top and middle). On August 12, the tracer from this region is found, together with the N-African one, over the area of Bulgaria, Romania and Ukraine, ahead of the frontal system crossing the Mediterranean: the joint tracer occupies a large band (Figures 13 and 14, middle), which crosses the Aegean Sea, the western Black-Sea, and continues to the NW over Poland into the Baltic Sea. This location coincides with the position of the water vapor front shown in both the MODIS data and the mesoscale model simulations (Figure 7, bottom). On August 13, during the final stage of the rainfall event in central Europe, the tracer emitted 3-to-4 days before from the Black Sea (Figure 14, bottom) moved into the northeastern border of the target area in central Europe, suggesting that evaporation from that region of the Black Sea could have been feeding the rainfall at the final stage of the episode. The exact location and quantification of the evaporative sources in this region are evaluated and mapped in a companion paper by *Gangoiti et al.* [2011].

[24] Thus, we can conclude that the intense rain episodes in the western Black Sea region from August 12 to 13, occurred when the N-Atlantic air mass moving across the Adriatic Sea and flowing in the trailing region of the frontal system advancing along the Mediterranean Sea and southern Europe (Figure 12, middle), was uplifted over the mountain ranges of the Balkan Peninsula and faced the Black Sea region. The air mass located over the Black Sea at that time, moved ahead of the frontal system transporting water vapor evaporated locally at the region (Figure 14, middle) and further away, within the sea-breeze convergence area of the Atlas Mountains (Figure 13, middle). Thus, the evaporative sources of the western Black Sea region episode had to be located in a vast region extending all along the western

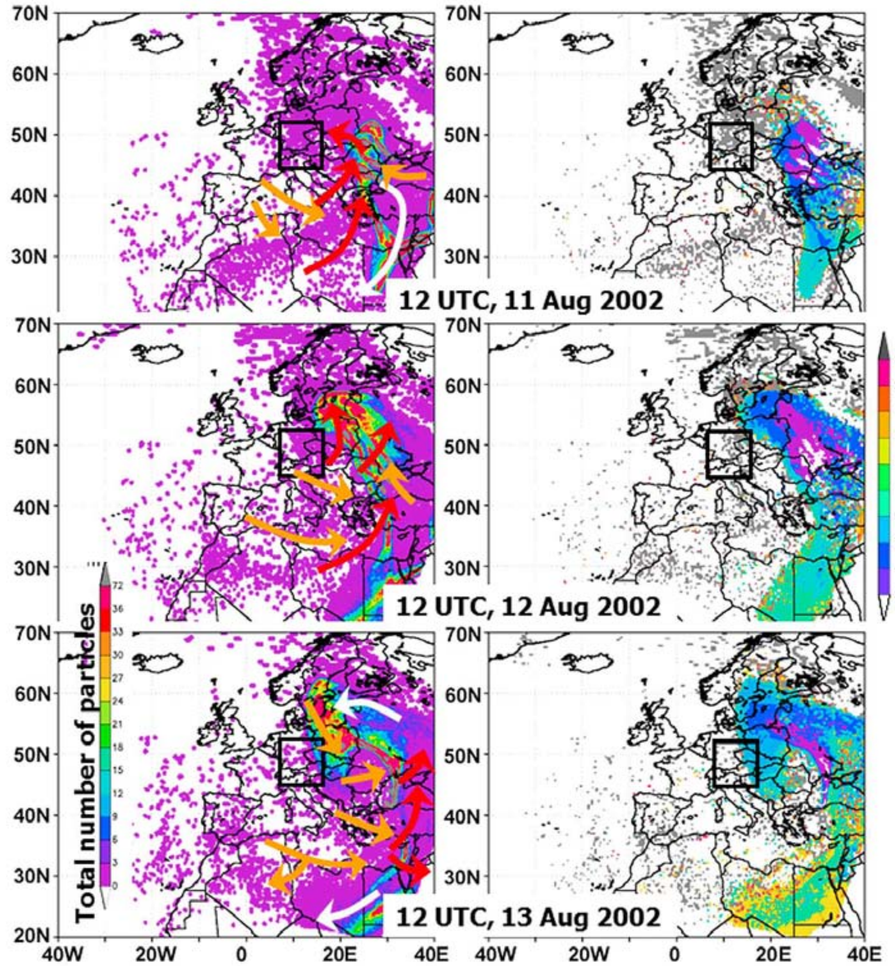

Figure 14. (left) Tracks of the Black Sea tracer (sources B1, B2 and B3 in Figure 3) during the rainfall maxima in central Europe from August 11 to 13, and (right) the age of the tracks. Like the N-African tracer in Figure 13, the Black Sea tracer did not penetrate into central Europe (the target area is marked with a black square) during the initial stages of the event (in the top panels). However, on August 12, at the beginning of the Black Sea rainfall events, this tracer is found (in the middle panels), together with the N-African tracer in Figure 13, over the area of Bulgaria, Romania and Ukraine, running ahead of the frontal system. During the final stage of the central Europe rainfalls, on August 13 (in the bottom panels), the tracers emitted 3–4 days before in the NW region of the Black Sea can be seen over the northeastern border of the target area in central Europe.

and central Mediterranean, northwestern Africa, probably including the subtropical Atlantic, and the landmass of southern Europe from Italy to the Black Sea.

[25] The target rainfall region of our search for water vapor sources was initially located in central Europe, and our mesoscale model domains were selected for the occasion. The size and resolution of the main domain appear reasonable for this investigation and although no conclusive statement can be drawn of possible, additional contributions from outside, the rainfall episode in the western Black Sea region seems to be affected by moisture sources located more to the south, outside the limit of grid #1: a large fraction of the N-African and the Black Sea tracers is being lost at this grid's southern boundary (Figures 13 and 14). This is not the case for the N-Atlantic air mass shown in Figure 12. Thus, the analysis and mapping of the contribution of the former regions to the rainfall episode in eastern Europe (the western Black Sea) will need to extend the main model domain to the south. Figure 15 documents the coverage of the circulations transporting the moisture from the tropical mid-troposphere to central and eastern Europe. Figures 15a and 15b show meridional moisture flux (vx specific humidity), averaged for the 2 periods of cyclone activity over the Mediterranean Sea observed during the first two weeks in August 2002: when the cyclonic midlatitude circulation is shifted to the south, affecting the Mediterranean area, large amounts of mid-troposphere moisture are released from the ITCZ and the subtropical environment northward. Once inserted in the cyclonic midlatitude circulation, the moisture can be released as precipitation. Alternatively, when the cyclone activity falls out of the area, as during the period August 6–9, the northward moisture flux is halted and the subtropical mid-troposphere moisture circulates around northern Africa (Figure 15c) in a similar

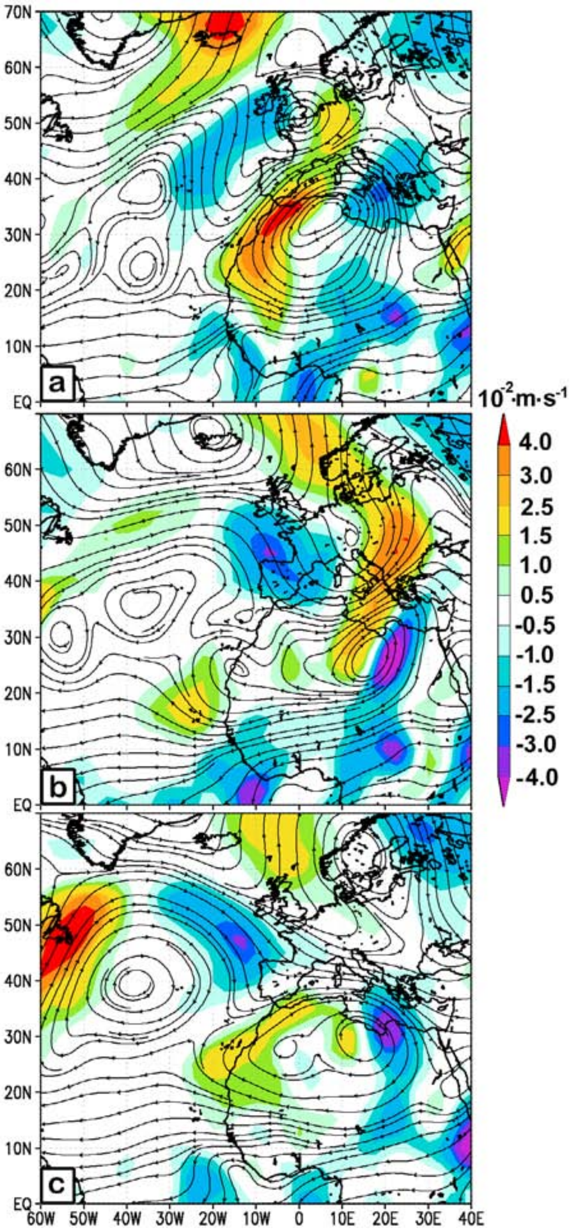

Figure 15. NCEP-reanalysis mean meridional moisture flux (1×10^{-2} ms^{-1}): red for northward flux and blue for southward) at the 600 hPa pressure level, averaged for 3 different periods: (a) 00 UTC August 3–18 UTC August 5, and (b) 00 UTC August 10–18 UTC August 12, correspond to the passage of cyclones over southern Europe and the western Mediterranean, and (c) 00 UTC August 6–12 UTC August 9 corresponds to a non-perturbed period (WMB accumulation period).

circulation to the one described by *Gangoiti et al.* [2006b], with implications in the transport of desert dust and European pollution. This type of long-range transport from the African ITCZ and the eastern Atlantic into Europe could also play an important role in the severe rainfall episodes that occur in the Mediterranean in autumn, as shown by *Turato et al.* [2004], when the Mediterranean becomes an active zone of cyclogenesis.

[26] Thus, it is evident that further applications of our methodology to evaluate the evaporative sources of these types of episodes will need larger domains, mainly enlarged to the south (transport from the tropical mid-troposphere) and to the west (transport from the N-Atlantic region, as discussed in the companion paper).

5. Conclusions

[27] The precipitation episode in August 2002 seemed to be caused by the concurrence of several ingredients needed for such an exceptional episode to happen: a) vapor accumulation in a large area in stably stratified layers within a non-precipitating environment, b) a convergence mechanism to bring all that vapor to a smaller domain (an upper-level trough, which deepened into a full scale depression as it encountered the moist and potentially unstable air mass accumulated over the WMB, provided the low level convergence and the upper-level divergence) and c) a frontal and orographic lifting in a mountainous region, which allowed the release of the accumulated moisture in a more reduced domain. It is also important to notice that, for this episode, the inland propagation of the rainfall events into an exceptionally large region was favored by the efficiency of the vapor transport after evapo-transpiration en route over lands already wet, which compensate the rainfall loses. This later feature resulted after consecutive precipitation episodes during a season characterized by midlatitude low tracks shifted more to the south, and crossing the Mediterranean area.

[28] Our analysis of the vapor accumulation from marine sources show that most of the precipitation taking place during the initiation of the central Europe rainfall episode (August 11–13, 2002) came from an air mass transported from the WMB. This air mass, initially of Atlantic origin, entered the Mediterranean through southern France over the Gulf of Lyon, and through northern Iberia channeled over the Ebro Valley. Once inside the basin, the western branch followed the combined upslope flows and coastal sea-breezes of eastern Iberia and northern Africa during the August 6–9 accumulation period, while the eastern branch drifted slowly southwards, parallel to the Italian Peninsula. Finally, on August 10, after the irruption of the Vb cyclone *Ilse* into the Mediterranean, the water vapor accumulated in the WMB was transported, through the Italian Peninsula and the Adriatic Sea, and across the western Balkans into the target area, initiating intense precipitations in central Europe on August 11. During the second half of the following day, a transition takes place from the Mediterranean origin of the air masses causing the rainfall, to an Atlantic origin. This change follows the irruption of air masses from the Atlantic in a direct NW-to-SE direction into the low pressure area developed on the target region. The colder Atlantic air masses were up-lifted by the mountain ranges located in southeastern Germany, and they faced the Mediterranean air masses inside the target region: the frontal system formed by the two air masses moved slowly across the target region to the East and caused intense precipitation until the early morning of August 13. Evapo-transpiration during the trajectory over the southeastern European landmass, before arriving at the precipitation areas on August 11, could have played an important role in increasing the available humidity for precipitation because of the presence of a moist land

surface (the entire region had already sustained important precipitations on August 6–7). Our mesoscale model results show that precipitation during the trajectory over the Balkans into the target area would have most likely compensated the evapo-transpiration, since the water vapor total column of the air mass causing severe rainfalls on August 11 remained constant from the Adriatic Sea to the target area. Terrestrial evaporative sources as well as their relative importance to marine sources are discussed by *Gangoiti et al.* [2011].

[29] The accumulation layers above the north-African convergence region, the eastern Mediterranean and the Black Sea seem to be more related to the intense rainfall events observed in wide areas of the Black Sea region (Bulgaria, Romania and Ukraine) during the second half of August 12 and 13. However, it is important to account that the caveat for this study is to have resorted to a limited area domain and time lapse. By the intrinsic definition of any regional model, the information from outside the domain comes from the boundary conditions. Whatever lies outside the boundaries is not part of the calculation: at this respect, when tracer trajectories cross the boundaries, nothing can be stated about their subsequent locations, even considering the fact that they could return back inside these boundaries if a larger domain and time lapse were selected.

[30] However, regardless of sources outside the domain, this study emphasizes the importance of subsidence over the WMB in the warm season as a prominent mechanism to accumulate moisture, that can be transported and released when a proper combination of forcings and triggering mechanisms are set in place. The same accumulation mechanisms could be relevant for other rainfall cases and they should be put into test. The implications for this important result are remarkable from the point of view of extreme precipitation forecasting in Europe.

[31] **Acknowledgments.** The authors wish to thank the Spanish Ministry of Science and Innovation (MICINN), for their financial support for the projects TRAMA (CGL2004–04448) and GRACCIE (CONSOLIDER 2010, CSD 2007–0067). Additional financing was provided by the European Commission's Sixth Framework Programme, CIRCE Integrated Project: Climate Change and Impact Research: the Mediterranean Environment (Project 036961). We also acknowledge the MODIS mission scientists and associated NASA personnel for the production of the data used in this research effort. We thank the Basque Service of Meteorology for providing the WPR data measured in the Port of Bilbao, Dominique Ruffieux from MeteoSwiss for the WPR data at Basel and B. Rudolf together with J. Rapp, from the German MetService, for allowing us to use their interpolation of surface rainfall data. Finally, the authors would like to acknowledge the comments and suggestions by Oreste Reale, during the completion process of the final form of this manuscript.

References

Anderson, J. R., E. E. Hardy, J. T. Roach, and R. E. Witmer (1976), A land use and land cover classification system for use with remote sensor data, *U.S. Geol. Surv. Prof. Pap.*, *964*, 28 pp.

Christensen, J. H., and O. Christensen (2003), Severe summertime flooding in Europe, *Nature*, *421*, 805–806, doi:10.1038/421805a.

Fricke, W., and U. Kaminski (2002), Ist die Zunahme von Starkniederschläen auf veränderte Wetterlagen zurückzuführen?, *GAW Brief Dtsch. Wetterdienstes*, *12*, 1–2.

Gangoiti, G., M. M. Millán, R. Salvador, and E. Mantilla (2001), Long-range transport and re-circulation of pollutants in the Western Mediterranean during the RECAPMA Project, *Atmos. Environ.*, *35*, 6267–6276, doi:10.1016/S1352-2310(01)00440-X.

Gangoiti, G., L. Alonso, M. Navazo, J. A. García, and M. M. Millán (2006a), North African soil dust and European pollution transport to America during the warm season: Hidden links shown by a passive tracer simulation, *J. Geophys. Res.*, *111*, D10109, doi:10.1029/2005JD005941.

Gangoiti, G., A. Albizuri, L. Alonso, M. Navazo, M. Matabuena, V. Valdenebro, J. A. García, and M. M. Millán (2006b), Sub-continental transport mechanisms and pathways during two ozone episodes in northern Spain, *Atmos. Chem. Phys.*, *6*, 1469–1484, doi:10.5194/acp-6-1469-2006.

Gangoiti, G., I. Gómez-Domenech, E. Sáez de Cámara, L. Alonso, M. Navazo, J. Iza, J. A. García, J. L. Ilardia, and M. M. Millán (2011), Origin of the water vapor responsible for the European extreme rainfalls of August 2002: 2. A new methodology to evaluate evaporative moisture sources, applied to the August 11–13 central European rainfall episode, *J. Geophys. Res.*, *116*, D21102, doi:10.1029/2010JD015538.

Gesch, D. B., K. L. Verdin, and S. K. Greenlee (1999), New land surface digital elevation model covers the earth, *Eos Trans. AGU*, *80*(6), 69–70, doi:10.1029/99EO00050.

Hanna, S. R., and R. Yang (2001), Evaluations of Mesoscale Model's simulations of near surface winds, temperature gradients and mixing depths, *J. Appl. Meteorol.*, *40*, 1095–1104, doi:10.1175/1520-0450(2001)040<1095:EOMMSO>2.0.CO;2.

Harrington, J. Y., T. Reisin, W. R. Cotton, and S. M. Kreidenweis (1999), Exploratory cloud-resolving simulations of Arctic stratus. Part II: Transition-season clouds, *Atmos. Res.*, *51*, 45–75, doi:10.1016/S0169-8095(98)00098-2.

Helfand, H. M., and J. C. Labraga (1988), Design of a nonsingular level 2.5 second-order closure model for the prediction of atmospheric turbulence, *J. Atmos. Sci.*, *45*, 113–132, doi:10.1175/1520-0469(1988)045<0113:DOANLS>2.0.CO;2.

James, P., A. Stohl, N. Spichtinger, S. Eckhardt, and C. Forster (2004), Climatological aspects of the extreme European rainfall of August 2002 and a trajectory method for estimating the associated evaporative source regions, *Nat. Hazards Earth Syst. Sci.*, *4*, 733–746, doi:10.5194/nhess-4-733-2004.

Kanamitsu, M., W. Ebisuzaki, J. Woollen, S. K. Yang, J. J. Hnilo, M. Fiorino, and G. L. Potter (2002), NCEP-DOE AMIP-II Reanalysis (R-2), *Bull. Am. Meteorol. Soc.*, *83*, 1631–1643, doi:10.1175/BAMS-83-11-1631.

Mellor, G. L., and T. Yamada (1982), Development of a turbulence closure model for geophysical fluid problems, *Rev. Geophys.*, *20*, 851–875, doi:10.1029/RG020i004p00851.

Millán, M. M. (2007), Climate/water-cycle feedbacks in the Mediterranean: The role of land-use changes and the propagation of perturbations at the regional and global scale, in *Regional Climate Variability and its Impacts in the Mediterranean Area*, *NATO ASI Ser.*, vol. 79, part 2, edited by A. Mellouki and A. R. Ravishankara, pp. 83–101, doi:10.1007/978-1-4020-6429-6_6.

Millán, M. M., B. Artíñano, L. Alonso, M. Castro, R. Fernandez-Patier, and J. Goberna (1992), Mesometeorological cycles of air pollution in the Iberian Peninsula (MECAPIP), *Air Pollut. Res. Rep. 44*, 219 pp., Eur. Comm., Brussels.

Millán, M. M., R. Salvador, E. Mantilla, and B. Artíñano (1996), Meteorology and photochemical air pollution in southern Europe: Experimental results from EC research projects, *Atmos. Environ.*, *30*, 1909–1924, doi:10.1016/1352-2310(95)00220-0.

Millán, M. M., R. Salvador, E. Mantilla, and G. Kallos (1997), Photo-oxidant dynamics in the Mediterranean basin in summer: Results from European research projects, *J. Geophys. Res.*, *102*(D7), 8811–8823, doi:10.1029/96JD03610.

Millán, M. M., et al. (2005), Climatic feedbacks and desertification: The Mediterranean model, *J. Clim.*, *18*, 684–701, doi:10.1175/JCLI-3283.1.

Mudelsee, M., M. Börngen, G. Tetzlaff, and U. Grünewald (2004), Extreme floods in central Europe over the past 500 years: Role of cyclone pathway "Zugstrasse Vb", *J. Geophys. Res.*, *109*, D23101, doi:10.1029/2004JD005034.

Pielke, R. A., et al. (1992), A comprehensive meteorological modelling system–RAMS, *Meteorol. Atmos. Phys.*, *49*, 69–91, doi:10.1007/BF01025401.

Reynolds, R. W., and T. M. Smith (1994), Improved global sea surface temperature analyses using optimum interpolation, *J. Clim.*, *7*, 929–948, doi:10.1175/1520-0442(1994)007<0929:IGSSTA>2.0.CO;2.

Rudolf, B., and J. Rapp (2003), The century flood of the River Elbe in August 2002: Synoptic weather development and climatological aspects, *Q. Rep. German NWP-Syst. 2, Part 1*, pp. 18–23, Dtsch. Wetterdienst, Offenbach am Main, Germany.

Tremback, C. J., W. A. Lyons, W. P. Thorson, and R. L. Walko (1993), An emergency response and local weather forecasting software system, in *Proceedings of the 20th ITM on Air Pollution and its Applications*, pp. 423–429, Springer, New York.

Turato, B., O. Reale, and F. Siccardi (2004), Water vapor sources of the October 2000 Piedmont flood, *J. Hydrometeorol.*, *5*, 693–712, doi:10.1175/1525-7541(2004)005<0693:WVSOTO>2.0.CO;2.

Ulbrich, U., T. Brücher, A. H. Fink, G. C. Leckebusch, A. Krüger, and J. G. Pinto (2003a), The central European Floods in August 2002, Part I: Rainfall periods and flood development, *Weather*, *58*, 371–376.

Ulbrich, U., T. Brücher, A. H. Fink, G. C. Leckebusch, A. Krüger, and J. G. Pinto (2003b), The central European Floods in August 2002, Part II: Synoptic causes and considerations with respect to climatic change, *Weather*, *58*, 434–441.

Walko, R. L., W. R. Cotton, M. P. Meyers, and J. Y. Harrington (1995), New RAMS cloud microphysics parameterization. Part I: The single-moment scheme, *Atmos. Res.*, *38*, 29–62, doi:10.1016/0169-8095(94)00087-T.

Walko, R. L., et al. (2000), Coupled atmospheric-biophysics-hydrology models for environmental modelling, *J. Appl. Meteorol.*, *39*, 931–944, doi:10.1175/1520-0450(2000)039<0931:CABHMF>2.0.CO;2.

Zhong, S., and J. Fast (2003), An evaluation of the MM5, RAMS, and Meso-Eta models at subkilometer resolution using VTMX field campaign data in the Salt Lake Valley, *Mon. Weather Rev.*, *131*, 1301–1322, doi:10.1175/1520-0493(2003)131<1301:AEOTMR>2.0.CO;2.

L. Alonso, G. Gangoiti, J. A. García, M. C. Gómez, J. L. Ilardia, J. Iza, M. Navazo, and E. Sáez de Cámara, Escuela Técnica Superior de Ingeniería de Bilbao, Universidad del País Vasco–Euskal Herriko Unibertsitatea, Alameda de Urquijo s/n, E-48013 Bilbao, Spain. (g.gangoiti@ehu.es)

M. M. Millán, Fundación CEAM, Charles Darwin 14, Parque Tecnológico, Paterna, E-46980 Valencia, Spain.